Ramirez Hoyos, P.; Cervera, J.; Manzanares, JA.; Nasir, S.; Ali, M.; Ensinger, W.; Mafe, S. (2022). Electrical conductance of conical nanopores: Symmetric and asymmetric salts and their mixtures. The Journal of Chemical Physics. 157(14):144702-1-144702-11. https://doi.org/10.1063/5.0119910

Electrical conductance of conical nanopores: symmetric and asymmetric salts and their mixtures

Patricio Ramirez[1,a)] Javier Cervera,[2] José A. Manzanares,[2] Saima Nasir,[3,4] Mubarak Ali,[3,4] Wolfgang Ensinger,[3] and Salvador Mafe[2]

[1]*Departament de Física Aplicada, Universitat Politécnica de València, E-46022 València (Spain)*
[2]*Departament de Física de la Terra i Termodinàmica, Universitat de València, E-46100 Burjassot (Spain)*
[3]*Department of Material- and Geo-Sciences, Technische Universität Darmstadt, D-64287 Darmstadt (Germany)*
[4]*Materials Research Department, GSI Helmholtzzentrum für Schwerionenforschung, D-64287 Darmstadt, Germany*

We have studied experimentally the electrical conductance-voltage curves of negatively and positively charged conical nanopores bathed by ionic solutions with monovalent, divalent, and trivalent cations at electrochemically and biologically relevant ionic concentrations. To better understand the interaction between the pore surface charge and the mobile ions, both single salts and salt mixtures have been considered. We have paid attention to the effects on the conductance of the cation valency, the pore charge asymmetry, and the pore charge inversion phenomena due to trivalent ions, both in single salts and salt mixtures. In addition, we have described how small concentrations of multivalent ions can tune the nanopore conductance due to monovalent majority ions, together with the effect of these charges on the additivity of ionic conductances and fluoride-induced negative differential conductance phenomena. This compilation and discussion of previously presented experimental data offers significant insights on the interaction between fixed and mobile charges confined in nanoscale volumes and should be useful to establish and check new models for describing ionic transport in the vicinity of charged surfaces.

[a)]Author to whom correspondence should be addressed: patraho@fis.upv.es

I. INTRODUCTION

The interaction between the mobile ions in aqueous solutions and the pore surface charges is central to ionic transport in membrane-based processes such as desalination and electrochemical energy conversion.[1-4]Also, this interaction regulates the electrophoresis of biological macromolecules such as DNA[5] and determines the ionic selectivity of the protein ion channels inserted in biomembranes.[6,7] Remarkably, the basic phenomena involved can be analyzed by using single-nanopore membranes under controllable laboratory conditions.[8-12]

We present a unified perspective of the electrical conductance of monovalent, divalent, and trivalent cations salts in both negatively and positively charged conical nanopores on the basis of recent experimental data.[12-16] Carboxylic acid groups provide the fixed charges $R–COO^-$ of the negatively charged pore at neutral pH.[17] Poly(allylamine hydrochloride) chains functionalized on the surface of this nanopore by electrostatic attachment provide the fixed charges $R–NH_3^+$ of the positively charged pore.[13] In the negative pore, monovalent (Li^+, Na^+, K^+), divalent (Ca^{2+}, Mg^{2+}, Ba^{2+}) and trivalent (Al^{3+}, Cr^{3+}, and La^{3+}) cations (*counterions*) are electrostatically attracted to the pore solution whereas in the positively charged pore these mobile ions (*coions*) are partially excluded from this solution.

The experimental data compiled and discussed here have been obtained at electrochemically and biologically relevant concentrations using biomimetic nanostructures whose high surface-to-volume ratio enhances the interaction between the mobile ions and the pore charges.[17] Note that the cations Li^+, Na^+, K^+, Ca^{2+}, and Mg^{2+}, together with the carboxylic acid and charged amino residues, are typical of the ion channel proteins inserted in the cell membrane.[6] Also, Ba^{2+} and La^{3+} are typical blockers of biological ion channels.[6,18-20]

Mixtures of salts with monovalent (KCl), divalent ($CaCl_2$, $MgCl_2$, $BaCl_2$) and trivalent ($LaCl_3$) cations[12,14] are also considered. In the last case, the screening of the negatively charged

pore groups by the trivalent cations can lead to charge inversion phenomena.[12,21-23] Remarkably, small amounts of multivalent ions can tune the electric current transported by majority monovalent ions.[14,15,23-25] We discuss also fluoride-induced negative differential conductance phenomena in conical nanopores[15] showing current drops with a peak-to-valley ratio of the order of 10, together with the problem of ionic conductance additivity,[16] are discussed.

While excellent general reviews describing basic phenomena and applications of nanopores have been published,[10,26-28] we believe that the compilation and discussion of our recent data focused on ionic conductances provide new physical insights on the interaction between fixed and mobile charges confined in nanoscale volumes, a problem of great interest also in biophysics.[5-7,29] Thus, this outlook should be useful to establish and check new models for describing ionic conductance in the vicinity of charged surfaces, a multidisciplinary problem relevant to biology, chemistry, and physics.

II. EXPERIMENTAL NANOPORE CHARACTERIZATION

We give a brief description of the experimental system before presenting and discussing the results obtained. A polyimide (PI) foil (Kapton50 HN, DuPont) 12.5-μm thick irradiated at the *UNILAC* linear accelerator (GSI, Darmstadt) by swift heavy ions (Au) of energy 11.4 MeV per nucleon forms the basis of the single-pore membrane used.[30,31] The irradiated membrane track is converted into a conical nanopore by asymmetric track-etching procedures.[30-32] Gold replicas of the resulting conical pores, SEM images of the pore fracture, and independent pore conductance measurements, suggest pore radii in the range 10–40 nm for the cone tip and 300–800 nm for the cone base.[17,33] The negative pore charges obtained at neutral pH values arise from the ionization of carboxylate residues obtained during the track-etching process (*samples 1* and *4–10*), leading to typical surface charge concentrations between −0.1 and −1.0 e/nm^2, with e the elementary charge.[17] Pore functionalization with positive poly(allylamine

hydrochloride) (PAH) chains is achieved by electrostatic attachment at neutral pH,[13] as shown in Fig. 1a (*samples 2* and *3*).

The current (I) – voltage (V) curves of the pore (Fig. 1b) and the conductance $G = I/V$ (Fig. 1c) are measured using a Keithley 6487 picoammeter-voltage source (Keithley Instruments, Cleveland, Ohio).[12] During the experiments, the aqueous solutions are kept at neutral pH values. Note that in this case the order of magnitude of the hydrogen concentration (10^{-7} M) is much lower than both the hydrogen concentration that would correspond to the typical pKa = 4 – 5 of the carboxylic acid groups at the pore surface and the ionic concentrations used here. Similarly, the temperature T is kept close to the laboratory ambient conditions (22 ^{o}C) so that the reference value $T = 295$ K can be taken for the experimental data. Input potentials and output currents are measured using Ag|AgCl electrodes,[12] with the reference electrode placed in the solution close to the pore base. Data reproducibility was found to be good, as shown previously.[13–16] For the negatively charged pore (*sample 1*), low electrical conductances are observed when the current enters the cone base at $V < 0$ while high conductances are obtained when the current enters the cone tip at $V > 0$.[17] The opposite case corresponds to the positively charged pore (*sample 2* obtained by the functionalization of *sample 1*). The electrical conductance $G – V$ curves obtained for the two pores are shown in Fig. 1c. The symmetry of these curves suggests an efficient conversion of the originally negative groups into positive groups, which allows a significant discussion of the mobile ions-pore charge interactions in the two cases.

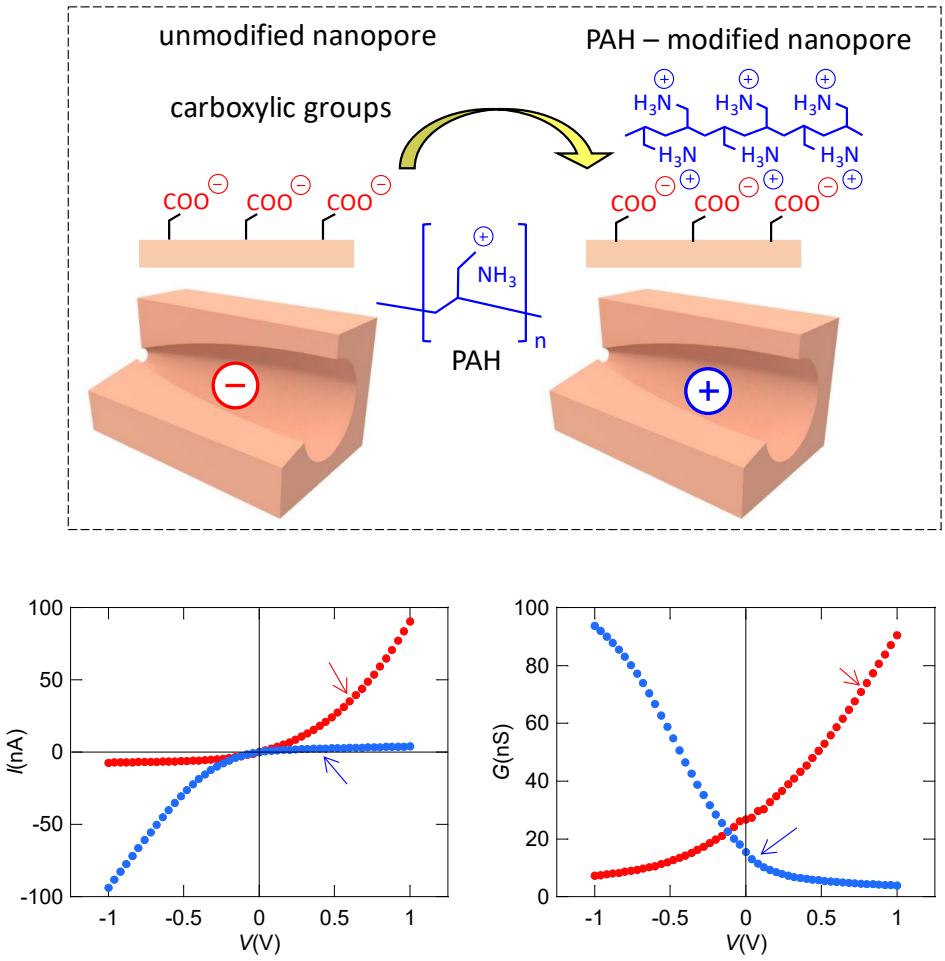

FIG. 1 (a) Conversion of the negatively charged to the positively charged pore by the surface functionalization of a positively charged polyelectrolyte achieved by electrostatic attachment.[13] (b) Current (I) – voltage (V) curves for the *sample 1* of the unmodified pore and *sample 2* of the PAH-functionalized pore measured at 100 mM KCl concentration.[13] (c) The corresponding conductance (G) – voltage (V) curves.

III. RESULTS AND DISCUSSION

A. Monovalent cations

Fig. 2 gives the $G - V$ curves obtained with the monovalent salts LiCl, NaCl, and KCl for the two single-pore membranes of Fig. 1. We focus our study on the high conductance regimes of the pore samples ($V > 0$ for *sample 1* and $V < 0$ for *sample 2*). For the negatively

and positively charged pores, the sequence of conductances qualitatively follows that of the diffusion coefficients in dilute solutions, $D_{K^+} = 1.957 > D_{Na^+} = 1.334 > D_{Li^+} = 1.029$, in units of 10^{-9} m^2/s for the three monovalent cations studied.[6] However, the positively charged pore shows more significant quantitative differences between the distinct cations than the negatively charged pore. This fact suggests that the different electrical nature of the cations, which are counterions in the case of the negatively charged pore but coions in the case of the positively charged pore, is important. Note also that, although the main carriers are anions rather than cations in the positively charged pore, the fact is that concentrations of the order of 100 mM are close to the effective pore charge concentration,[17] which may give a moderate coion exclusion only. Thus, a quasi-electroneutral solution of mobile ions could exist over a significant fraction of the pore volume.

In the negatively charged pore, the cations tend to be close to the pore surface in order to compensate for the fixed charges. In the positively charged pore, however, they are repelled by the pore surface and tend to reside in the approximately electroneutral solution at the pore center where the distinct ionic diffusion coefficients result in different quasi-electroneutral solution conductions. Note that the differences between the negatively and positively charged pore conductances for the distinct cations may reflect also specific interactions between these cations and the different functional groups on the pore surface.

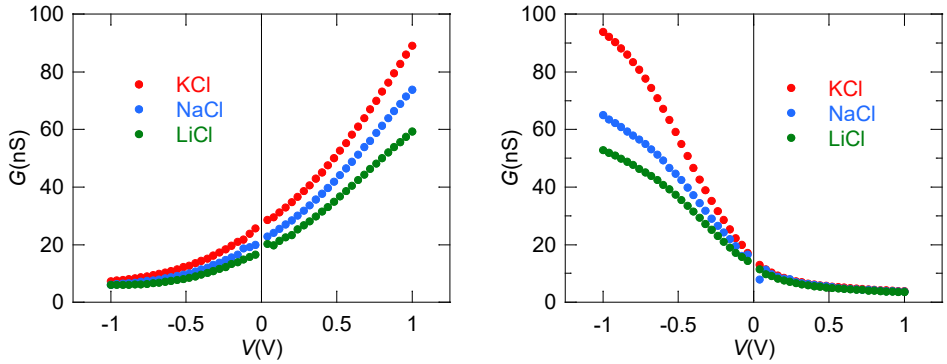

FIG. 2 (a) Conductance (G) – V curves of the negatively charged unmodified pore *(sample 1*) of Fig. 1 for three 1:1 salts with different monovalent cations and a common anion (Cl^-) at 0.1 M concentration. (b) $G - V$ curves for the positively charged pore (*sample 2*) of Fig. 1. The curves were obtained from the data of Ref. 13.

B. Divalent cations

Fig. 3 shows the $G - V$ curves of 2:1 salts of different divalent cations with a common anion. These cations are *counterions* in the negatively charged nanopore and *coions* in the positively charged nanopore. Note the relatively small voltage-induced changes and differences between the cations in the case of the negative pore with respect to the positively charged pore where the divalent cations act as *coions* rather than *counterions* compensating for the pore charges. In the positively charged pore, the conductance differences are especially significant for $MgCl_2$, corresponding to the more hydrated Mg^{2+} ion in respect to the cases of Ca^{2+} and Ba^{2+}. This fact may suggest again that the small differences between ionic diffusion coefficients are more noticeable in the bulk solution at the center of the pore. Note again that, although the main carriers are anions rather than cations in the positively charged pore, the coion exclusion effect is only moderate at concentrations of the order of 100 mM,[17] so that a quasi-electroneutral solution of mobile ions should exist at the pore center.

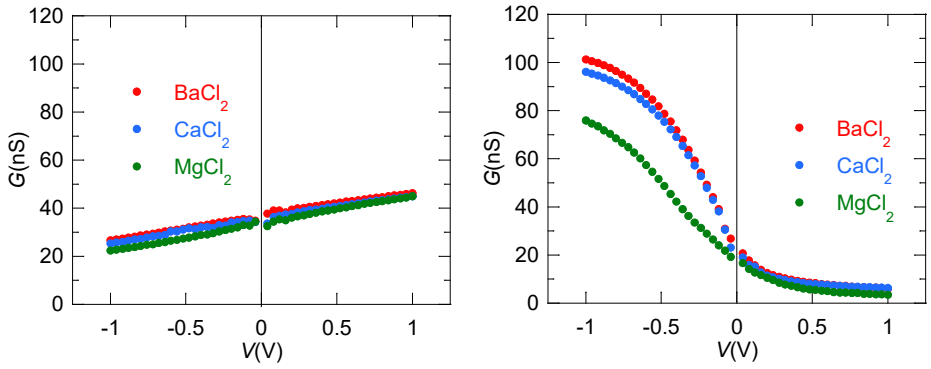

FIG. 3 (a) $G - V$ curves of the negatively charged unmodified pore *(sample 1*) of Fig. 1 for three 2:1 salts with different divalent cations and a common anion (Cl^-) at 0.1 M. (b) $G - V$ curves for the positively charged pore (*sample 2*) of Fig. 1. The curves were obtained from the data of Ref. 13.

C. Trivalent cations

The case of trivalent cations is considered in Fig. 4 for the unmodified pore (*sample 1*) and a new PAH-functionalized pore (*sample 3*) for three 3:1 chloride salts. The significant change observed in the sign of the current rectification ratio for the unmodified pore with respect to the pure KCl case included for comparison suggests that a significant amount of trivalent cations (La^{3+}, Al^{3+} and Cr^{3+}) are now located in the immediate vicinity of the originally negative pore surface. The resulting overcompensation of the fixed charges can convert the negative pore into a positively charged pore (Fig. 4a) exhibiting similar rectification to that of the PAH-functionalized pore (Fig. 4b).[13]

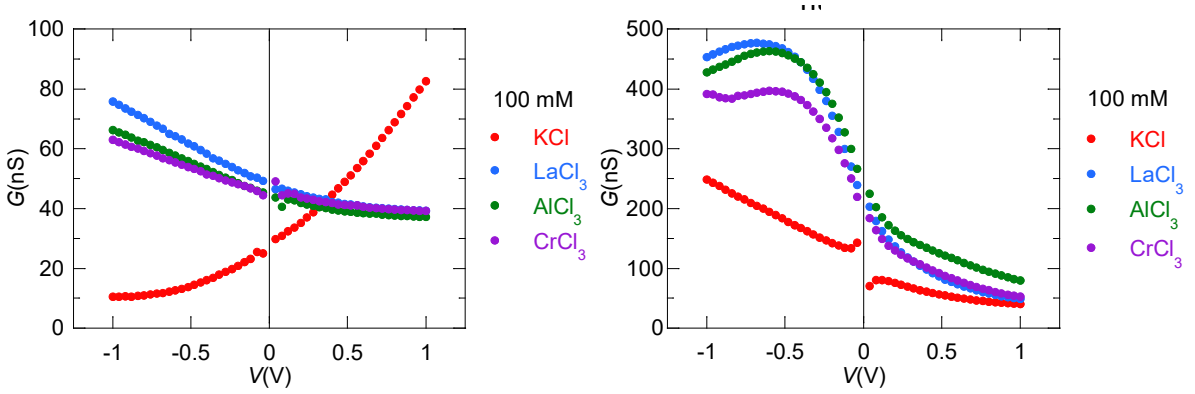

FIG. 4 (a) $G - V$ curves of the negatively charged pore (*sample 1*) and three 3:1 salts with different trivalent cations and a common anion (Cl^-) at 0.1 M concentration. The case of the 1:1 KCl salt is included for comparison. (b) $G - V$ curves for the positively charged pore (*sample 3*). The curves were obtained from the data of Ref. 13.

Charge inversion is usually reported for charged colloids electrophoresis in solutions of multivalent ions,[34,35] as well as in atomic force microscopy[36] and X-ray reflectivity[37] measurements. In addition, it can be detected by the changes in the ionic selectivity of biological ion channels.[19,23] Interestingly, charge inversion phenomena in the presence of calcium cations were demonstrated for the negatively charged C-terminus of a protein captured in the VDAC nanopore of a neutral lipid membrane,[38] suggesting that charge inversion can take place at the level of a single polypeptide chain. Charge inversion can also be studied by means of computer simulations in strongly correlated liquids of multivalent ions in the vicinity of charged surfaces.[34,35,39-41]

After considering the single salts case, Figs. 5a–5f give a complete experimental account of the conductance observed in negatively charged pores for salt mixtures of $LaCl_3$ and KCl. Remarkably, small amounts of La^{3+} significantly change the conductance and rectification of the negative pore, suggesting again that small concentrations (5 mM) of trivalent ions not only screen the negative fixed charges but can also overcompensate them to give an effectively positively charged pore. Fig. 5 also shows that adding KCl decreases the above charge reversal

effect because of the competition between the two cations for the pore charges and the enhanced screening of the positive fixed charges, thus giving significant changes in the rectification ratio. A theoretical model for the pore charge inversion in salt mixtures based on the Nernst-Planck equations has been given previously.[12] The model provides qualitative explanations for the effect of the pore charge overcompensation by La^{3+} ions.

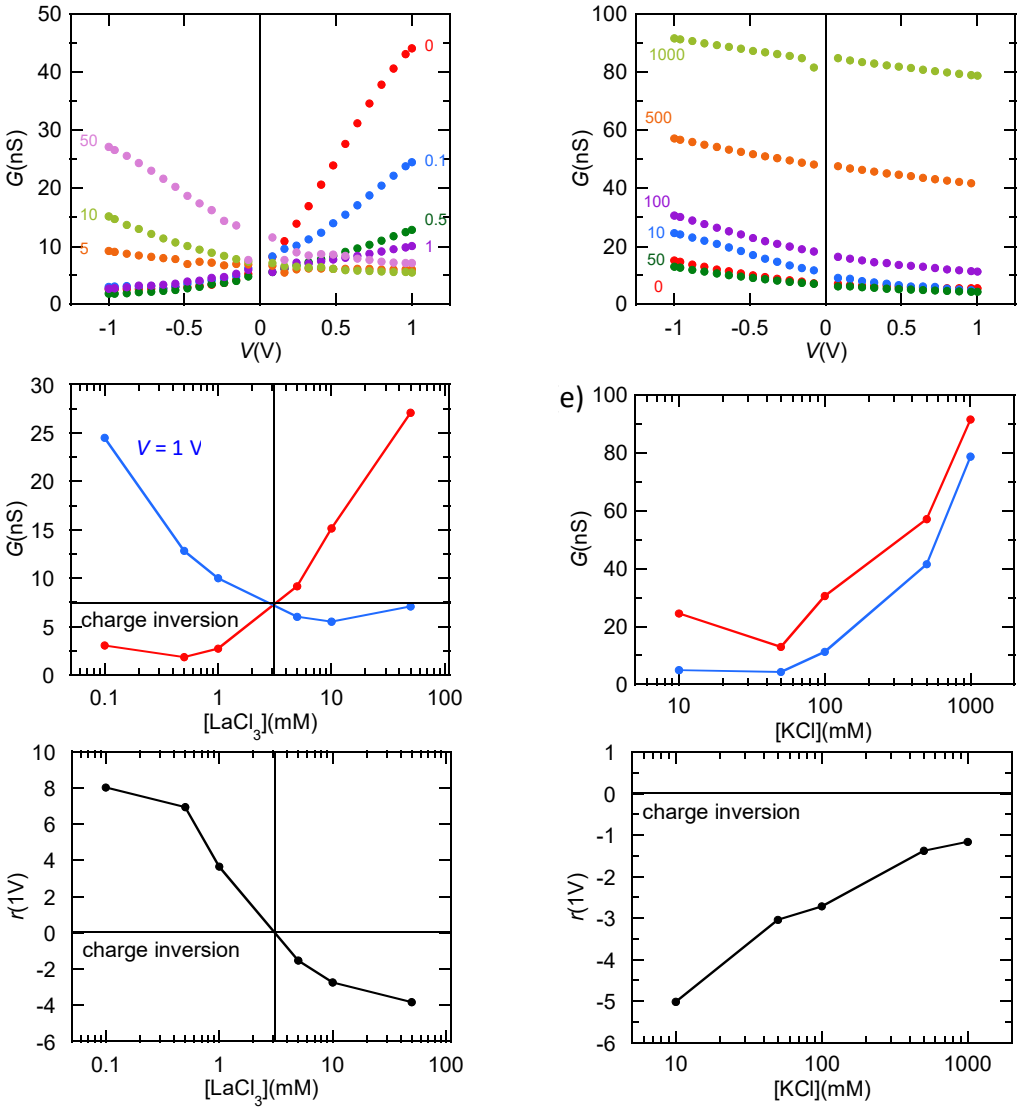

FIG. 5 (a) $G - V$ curves of monovalent and trivalent cation mixtures parametrically in the $LaCl_3$ concentration at fixed 50 mM KCl for pore *sample 4*. (b) The corresponding G values as a function of the $LaCl_3$ concentration at two fixed voltages V = +1 and = –1 V. (c) The

corresponding rectification current ratios $r(V = 1\ \text{V})$, defined as the *absolute value* of $I(V = 1\ \text{V})/I(V = -1\ \text{V})$ for positive ratios and as $I(V = -1\ \text{V})/I(V = 1\ \text{V})$ for negative ratios, clearly show the charge inversion. (d) $G - V$ curves of monovalent and trivalent cation mixtures parametrically in the KCl concentration at fixed 50 mM $LaCl_3$ for pore *sample 4*. (e) The conductances as a function of the KCl concentration at the two above voltages. (f) The corresponding rectification ratios suggest charge inversion for all KCl concentrations. The curves were obtained from the data of Ref. 12.

D. Salt mixtures

Fig. 6 explores the non-monotonic conductances that can be observed in negatively charged pores and salt mixtures where the divalent cations Mg^{2+}, Ba^{2+}, and Ca^{2+} coexist with the monovalent cation K^+ and the common anion Cl^- at pH = 7. Fig. 6a shows that G decreases with the concentration of $MgCl_2$ at low concentrations, eventually reaching a minimum. Again, this observation suggests that Mg^{2+} strongly interacts with the ionized carboxylic acid groups, and then the absolute value of the negative pore charge decreases. On the contrary, G increases quasi-linearly with the concentration of $MgCl_2$ at high concentrations, suggesting a dominant bulk conduction regime similar to that of an electroneutral solution.[42,43] In this case, the wide availability of mobile ions in the pore solution effectively screens the negative pore charges.[12,17]

As expected, because the pore asymmetry gives significantly different axial concentration profiles at $V < 0$ and $V > 0$,[17] no conductance minimum is observed for the negative voltage $V = -1$ V (Fig. 6a, *inset*). The shift of the conductance minimum to higher concentrations when the voltage is increased from $V = 1$ V to $V = 2$ V (Fig. 6a) is also a direct consequence of the potential-dependent concentration profiles along the axial position.[17] In particular, the decreased concentrations of the mobile ions give lower conductances for $V < 0$ than for $V > 0$, as explained with detail in Fig. 3 of Ref. 17. Note that this ionic depletion decreases the Debye screening of the pore fixed charges.

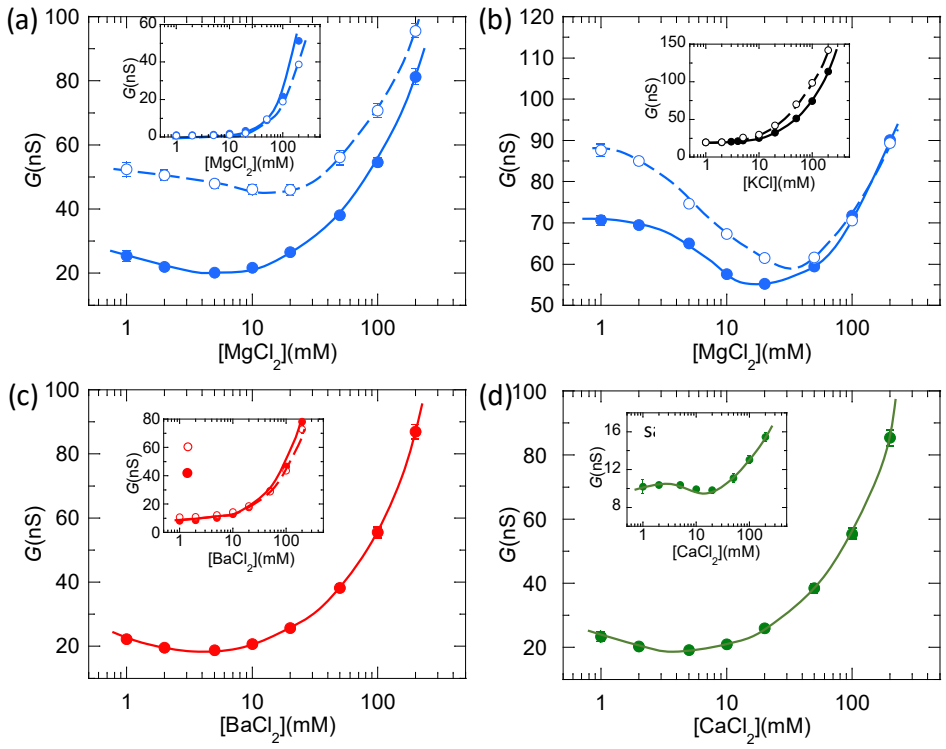

FIG. 6 (a) The conductances of a negatively charged nanopore (*sample* 5) at $V = 1$ V and 2 V as a function of the $MgCl_2$ concentration (G – $MgCl_2$ concentration curves) at fixed 10 mM KCl. The inset shows the conductances at $V = -1$ V and –2 V. (b) G – $MgCl_2$ concentration curves for $V = 1$ V and 2 V at 50 mM KCl for pore *sample 5*. The inset shows the G – KCl concentration curves for $V = 1$ V and 2 V at 10 mM $MgCl_2$ for pore *sample 5*. (c) G – $BaCl_2$ concentration curve for $V = 1$ V at 10 mM KCl. The *inset* shows the case of pH = 3, which gives a neutral pore, for $V = 1$ V and 2 V for pore *sample 5*. (d) G – $CaCl_2$ concentration curve for $V = 1$ V at 10 mM KCl for pore *sample 5*. For a different negatively charged pore (*sample* 6) the *inset* also shows a conductance minimum. In all cases, the error bars give the mean square deviations obtained from three independent measurements. The curves were obtained from the data of Ref. 14.

Fig. 6b indicates that, when the KCl concentration is kept to 50 mM instead of 10 mM, the conductance minimum is shifted to higher $MgCl_2$ concentrations with respect to Fig. 6a. In this case, the higher KCl concentration screens more effectively the negative pore charge, so that higher $MgCl_2$ concentrations are needed to decrease the absolute value of the pore charge. When we change the KCl concentration at constant 10 mM $MgCl_2$ (Fig. 6b, inset), no minimum

is observed, in agreement with the fact that the pore charge regulation is due to divalent rather than monovalent cations.

The above results clearly show that relatively small amounts of divalent cations can tune the effective pore charge. Remarkably, this fact leads to a counter-intuitive effect in the surface-regulated conductance regime where G decreases rather than increases with the divalent cation salt concentration, as confirmed also for other divalent cations (Ba^{2+} in Fig. 6c and Ca^{2+} in Fig. 6d). Consistent with these pore charge-based effects, Fig. 6c (*inset*) shows no conductance minimum for the case of a neutral pore: at pH = 3 most of the carboxylic groups are not ionized,[17,31] and thus the interaction between the divalent cations and the pore charges is negligible. Note also that the pore charge regulation of G is a robust effect that can be observed not only with different salts (Figs. 6a, 6c, and 6d) but also with distinct nanopores (Fig. 6d, *inset*). A qualitative theoretical model for the pore charge regulation by multivalent ion mixtures, which is based on the divalent cation adsorption and the Donnan distribution equilibria relating the external and pore ionic concentrations, can be found in Ref. 14.

Fig. 7 shows the conductance of a negatively charged pore (*sample* 5) at V = 1 V in mixtures of 10 mM KCl and a wide range of $MgCl_2$, $CaCl_2$ and $BaCl_2$ concentrations, 1 – 200 mM. The error bars clearly show the reproducibility and significance of the experimental conductances obtained for the divalent salts $MgCl_2$, $CaCl_2$ and $BaCl_2$ of Fig. 6. We may tentatively ascribe the opposite conductance orders consistently observed in the low and high divalent cation concentration regimes to: (*i*) the differences in the counterion cation hydration[6,42] and (*ii*) the majority ion that mostly contributes to G, either K^+ or the divalent cation depending on the concentration range.

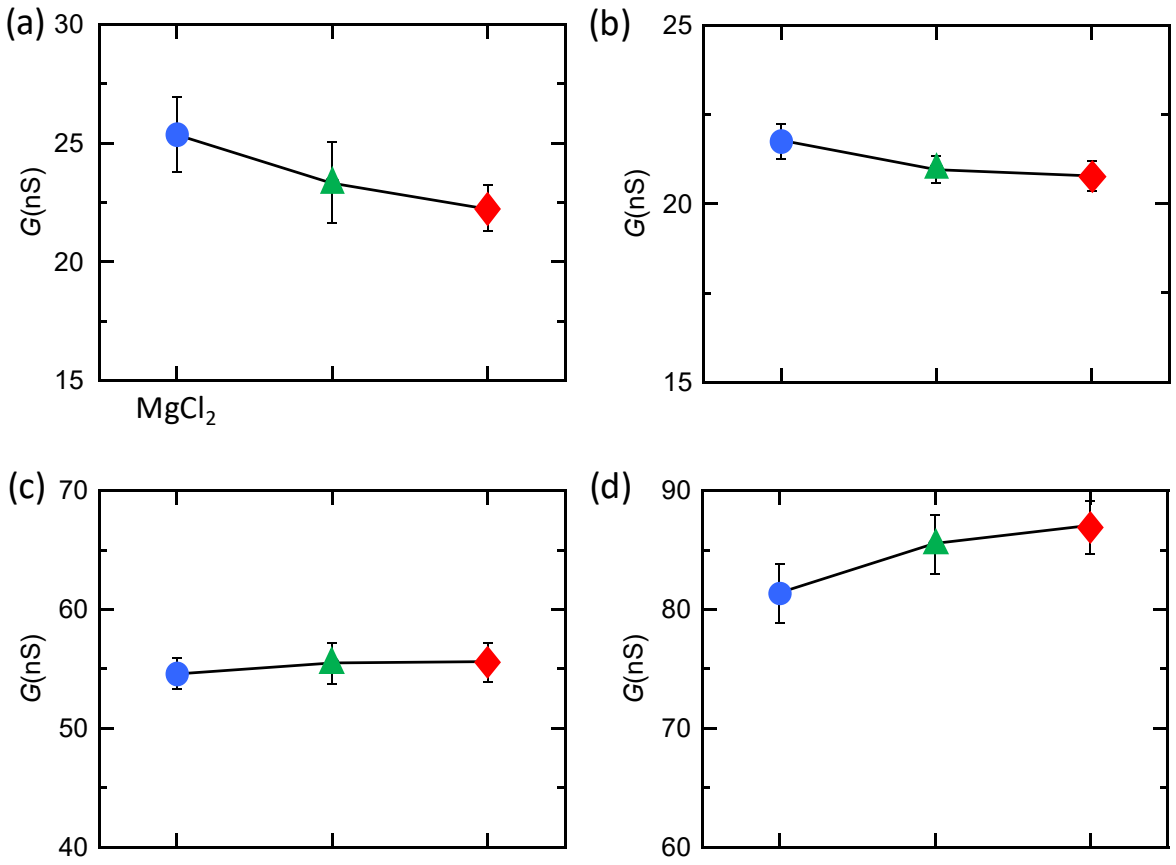

FIG. 7 The conductances G at fixed voltage $V = 1$ V for salt mixtures of 10 mM KCl and (a) 1 mM, (b) 10 mM, (c) 100 mM, and (d) 200 mM concentrations of $MgCl_2$, $CaCl_2$ and $BaCl_2$ (Fig. 6, pore *sample 5*). The error bars show the mean square deviations resulting from three independent measurements. The curves were obtained from the data of Ref. 14.

As to hydration, note that the Pauling radii and the water substitution rates around the divalent cations follow the increasing order $Mg^{2+} < Ca^{2+} < Ba^{2+}$, contrary to the hydration energies that follow the decreasing order $Mg^{2+} > Ca^{2+} > Ba^{2+}$.[6] Thus, the smaller naked counterion (Mg^{2+}) is more hydrated than the larger naked counterion (Ba^{2+}), which suggests that the strength of the electrical interaction of the divalent cations with the negative pore charge groups should increase in the order $Mg^{2+} < Ca^{2+} < Ba^{2+}$. Accordingly, at low divalent cation concentration, the effective pore charge concentration and then the majority ion (K^+)

concentration should be higher for Mg^{2+} than for Ba^{2+}. Thus, the conductance decreases following the series $G(Mg^{2+}) > G(Ca^{2+}) > G(Ba^{2+})$ in this low concentration regime, as observed experimentally (Figs. 7a and 7b). On the contrary, because of the increased Debye screening, the pore surface charges do not determine the conductance in the high concentration regime where the divalent cation rather than K^+ is the majority ion. In the bulk conduction corresponding to the high concentration regime, the more hydrated cation (Mg^{2+}) is the more retarded one due to the hydrodynamic friction with the aqueous media, which gives the opposite conductance order $G(Mg^{2+}) < G(Ca^{2+}) < G(Ba^{2+})$, as observed experimentally (Figs. 7c and 7d). Taking together, the above experimental facts demonstrate that divalent cations can regulate the effective pore charge and conductance of nanofluidic pores at low concentrations.[14,43-45]

In a different experimental context, it has been found that mixtures of two electrolytes at constant total concentration in protein ion channels have given a minimum current for a particular mole fraction, the so-called anomalous mole fraction effect (AMFE).[46] This effect has been ascribed to coordinated single filing effects in narrow pores[6] and to the binding of divalent cations giving depletion zones of mobile ions in wider pores.[46-48]

Other mixtures with a different cation are shown in Fig. 8 where new experimental data for the arrangements LiCl/$MgCl_2$ and $MgCl_2$/LiCl at low (2 mM) and high (100 mM) concentrations are presented. We observe that the pore conductance is maximum when the most conductive salt (LiCl) faces the pore tip, as expected from the generic $I - V$ curve of Fig. 1b. Note also the increased screening of the pore charges by the divalent cations with respect to the monovalent cations. The effect of the nanopore orientation is due to the asymmetric distribution of the conical pore fixed charges.[17]

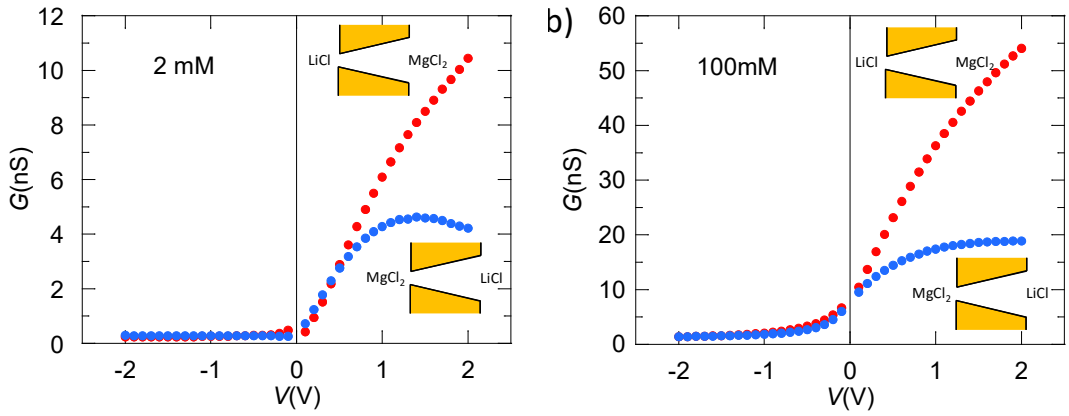

FIG. 8. (a) $G - V$ curves for the cases LiCl/$MgCl_2$ and $MgCl_2$/LiCl at low (2 mM) concentrations measured with a negatively charged pore (pore *sample 7*). (b) The same cases at high (100 mM) concentrations (pore *sample 7*).

E. Fluoride salts and negative differential conductance

Recently, fluoride-induced negative differential conductance phenomena in polyimide (PI) conical nanopores have been reported.[15] Nanoscale current drops with a peak-to-valley ratio of the order of 10 and threshold voltages around 1 V were observed in single pore and multipore samples with different pore radii and charge concentrations. The phenomena were studied for different salt concentrations, solvents, and cations[15] suggesting that the negative conductance effect occurs only for F^- ions and low concentrations in the mM range. Remarkably, the threshold voltage increased in the order V_{TH}(LiF) < V_{TH}(NaF) < V_{TH}(KF) (Fig. 9), following the inverse of the cation hydration energies.

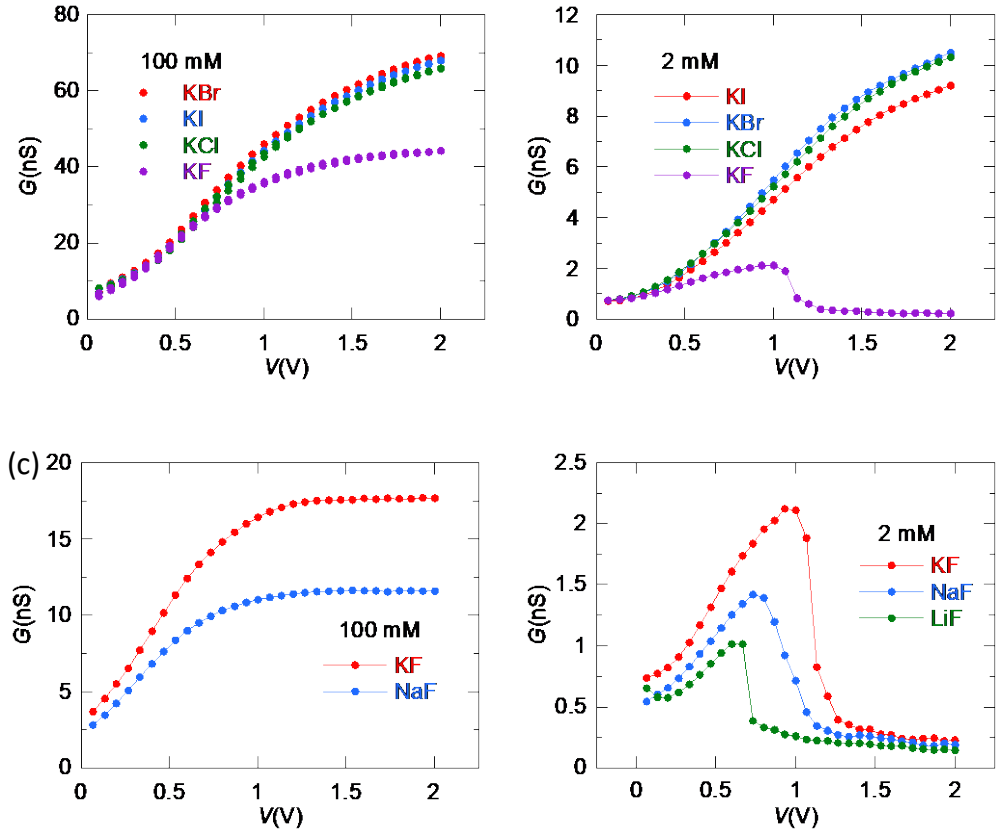

FIG. 9. (a) $G - V$ curves for the halide salts KI, KBr, KCl, and KF at 100 mM concentration (pore *sample 8*). (b) The $G - V$ curves at low (2 mM) concentrations (pore *sample 8*). (c) $G - V$ curves for NaF and KF at 100 mM concentration for a different negatively charged pore (*sample 9*). (d) $G - V$ curves for LiF, NaF, and KF at 2 mM concentration for pore *sample 9*. The curves were obtained from the data of Ref. 15.

Note that the F^- ion has a small ionic radius compared with those of the Cl^-, Br^-, and I^- ions. This fact suggests high surface charge density and hydration energy and thus a strong immobilization of the neighboring water molecules in confined nanoscale environments in the case of the F^- ion. Also, the pore tip radius can be of the same order of magnitude as the Debye length (about 10 nm) for 1–10 mM salt concentrations, which should decrease the Debye screening of the pore charge. Taken together, these conditions should compromise bulk ionic conduction, which is characterized by an excess of water molecules in dilute free solutions, in

the case of the narrow pore tip, thus suggesting a mixed pore surface and bulk conduction regime in our case.[15] The mobile cations dominate the conductance in the vicinity of the negative pore charges that exclude anions. In the pore center, however, bulk conduction can be dominant because the pore charges are effectively screened by the cations. In this context, the negative differential conductance effect should arise when the contribution of the surface conductance is significant compared with the pore center bulk conductance, as shown by the model results.[15] Note here that positively charged pores do not show negative conductance,[15] which suggests indeed that the negatively charged pore tip acts as a kinetic barrier for the F^- ion transport. The theoretical results based on the above two-region conductance model provided qualitative explanations for most of the observed phenomena, as shown previously.[15]

F. Additivity of ionic conductances

Kohlrausch's law of independent ionic migration establishes the decomposition of the molar conductivity Λ of a dilute electrolyte solution in ionic contributions. The relation $\Lambda_{KCl} + \Lambda_{NaA} = \Lambda_{NaCl} + \Lambda_{KA}$, where A^- is an anion different from Cl^-, is a consequence of this law.[49] Although Λ is a local quantity and G is an integral property, the conductance G of a nanopore is a sum of ionic contributions and the relation $G_{KCl} + G_{NaA} = G_{NaCl} + G_{KA}$, which shows some similarity with the Kohlrausch's law, may be satisfied[16] because the pore geometry factors are the same for all electrolytes.

Fig. 10 suggests that the relation $G_{KCl} + G_{NaA} = G_{NaCl} + G_{KA}$ is indeed approximately valid because the absolute values of the relative difference index $\Delta I \equiv [(G_{KCl} + G_{NaA}) - (G_{NaCl} + G_{KA})]/[(G_{KCl} + G_{NaA}) + (G_{NaCl} + G_{KA})]$ are of the order of 1% at the individual concentrations c_0 = 5, 20, and 50 mM. Note however that the physico-chemical rationale of this experimental fact is different in *free* electrolyte solutions and in nanopores. In the low concentration regime of Fig. 10, the anions Cl^- and A^- are excluded from the negatively charged pore and only the

cations K^+ and Na^+ significantly contribute to the ionic conduction. Therefore, the above relation is due to the anion exclusion from pores with negative charges and not to Kohlrausch's law of independent ionic migration, which applies only to free electrolyte solutions.

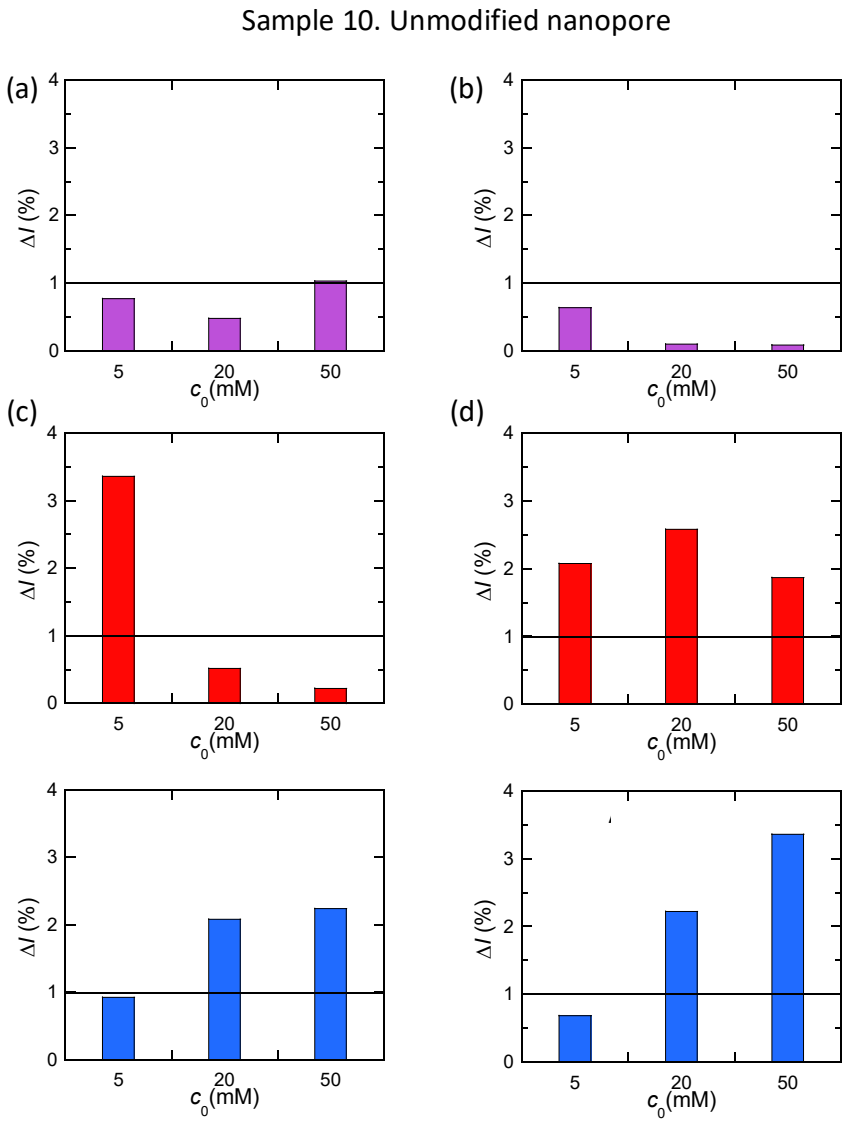

FIG. 10. Absolute values (in percentage) of the conductance ratio index $\Delta I \equiv [(G_{KCl} + G_{NaA}) - (G_{NaCl} + G_{KA})] / [(G_{KCl} + G_{NaA}) + (G_{NaCl} + G_{KA})]$ at voltages $V = 2$ V and -2 V for a negatively charged pore (*sample 10*). The electrolyte concentrations $c_0 = 5$, 20, and 50 mM are considered for the anions $A^- = I^-$ (a, b), F^- (c, d), and ClO_4^- (e, f). Data taken from Ref. 16.

IV. CONCLUSIONS

Studies on the conductance of nanopores and ion channels tend to emphasize the pore shape and negative surface charge effects,[50,51] usually focusing on salt concentration-dependent phenomena with pure salts of monovalent ions.[17,52-56] As a complementary view, we have given a detailed discussion of the effects of the cation valency on the electrical conductance of negatively and positively charged nanopores on the basis of a compilation of previously presented experimental data. To this end, electrochemically and biologically relevant ionic concentrations have been used both in single salts and in salt mixtures. Thus, we believe that this conductance-focused perspective gives significant insights on the interaction between fixed and mobile charges confined in nanoscale volumes and should be useful to establish and check new models for describing ionic transport in the vicinity of charged surfaces.[4,40,44,55-57]

The role of the valency on the transport rates of cations acting either as pore *counterions* or *coions*, together with the voltage, pore charge, and salt concentration effects, have been established. For monovalent ions, the ionic diffusion coefficients dominate ionic transport, resulting in a bulk-like conduction. For divalent cations however, the screening of the pore charges by the mobile ions becomes more noticeable, suggesting a mixed surface and bulk conduction. For trivalent cations, pore charge overcompensation can arise.

Also, we have discussed how small concentrations of multivalent ions can tune the nanopore conductance because of their electrical interaction with the pore charges, the effect of these charges on the additivity of ionic conductances, and the fluoride-induced negative differential conductance phenomena observed in conical nanopores, which should have practical implications for sensing procedures.

ACKNOWLEDGMENTS

P.R., J.C., J.A.M., and S.M. acknowledge the support from the *Ministerio de Ciencia, Innovación y Universidades* (Spain) and the *European Regional Development Funds* (FEDER),

project No. PGC2018-097359-B-100. M.A., S.N, and W.E. acknowledge the funding from the Hessen State Ministry of Higher Education, Research and the Arts, Germany, under the LOEWE project iNAPO.

DATA AVAILABILITY

The data that support the findings of this study are available from the corresponding author upon reasonable request.

AUTHOR DECLARATIONS

The authors have no conflicts of interest to disclose.

REFERENCES

[1]T. Luo, S. Abdu, and M. Wessling, Selectivity of ion exchange membranes: A review, J. Membrane Sci. **555**, 429 (2018).

[2]J. P. Hsu, S. C. Lin, C. Y. Lin, and S. Tseng, Power generation by a pH-regulated conical nanopore through reverse electrodialysis, J. Power Sources **366**, 169 (2017).

[3]S. Balme, T. Ma, E. Balanzat, and J. M. Janot, Large osmotic energy harvesting from functionalized conical nanopore suitable for membrane applications, J. Power Sources **544**, 18 (2017).

[4]A. Yaroshchuk, Transport properties of anti-symmetrically charged nanochannels in symmetrical electrolyte solutions, Microfluid. Nanofluid. **26**, 51 (2022).

[5]B. Luana and A. Aksimentiev, Electric and electrophoretic inversion of the DNA charge in multivalent electrolytes, Soft Matter **6**, 243 (2010).

[6]B. Hille, Ion channels of excitable membranes, Sinauer Associates, Sunderland, 1992.

[7]J. Cervera, A. Pietak, M. Levin, and S. Mafe, Bioelectrical coupling in multicellular domains regulated by gap junctions: a conceptual approach. Bioelectrochem. **123**, 45 (2018).

[8]E. Secchi, A. Niguès, L. Jubin, A. Siria, and L. Bocquet, Scaling Behavior for Ionic Transport and its Fluctuations in Individual Carbon Nanotubes, Phys. Rev. Lett. **116**, 154501 (2016).

[9]P. M. Biesheuvel and M. Z. Bazant, Analysis of ionic conductance of carbon nanotubes, Phys. Rev. E **94**, 050601(R) (2016).

[10]H. Zhang, Y. Tian, J. Hou, X. Hou, G. Hou, R. Ou, and H. Wang, L. Jiang, Bioinspired smart gate-location-controllable single nanochannels: experiment and theoretical simulation, ACS Nano **9**, 12264 (2015).

[11]G. Perez-Mitta, A. G. Albesa, M. E. T. Molares, C. Trautmann, and O. Azzaroni, The influence of divalent anions on the rectification properties of nanofluidic diodes: Insights from experiments and theoretical simulations, ChemPhysChem **17**, 2718 (2016).

[12]P. Ramirez, J. A. Manzanares, J. Cervera, V. Gomez, M. Ali, I. Pause, W. Ensinger, and S. Mafe, Nanopore charge inversion and current-voltage curves in mixtures of asymmetric electrolytes, J. Membrane Sci. **563**, 633 (2018).

[13]S. Nasir, M. Ali, J. Cervera, V. Gomez, M. H. Ali Haider, W. Ensinger, S. Mafe, and P. Ramirez, Ionic transport characteristics of negatively and positively charged conical nanopores in 1:1, 2:1, 3:1, 2:2, 1:2, and 1:3 electrolytes, J. Colloid Interface Sci. **553**, 639 (2019).

[14]P. Ramirez, J. A. Manzanares, J. Cervera, V. Gomez, M. Ali, S. Nasir, W. Ensinger, and S. Mafe, Surface charge regulation of functionalized conical nanopore conductance by divalent cations and anions, Electrochim. Acta **325**, 134914 (2019).

[15]J. J. Perez-Grau, P. Ramirez, V. Garcia-Morales, J. Cervera, S. Nasir, M. Ali, W. Ensinger, and S. Mafe, Fluoride-Induced Negative Differential Resistance in Nanopores: Experimental and Theoretical Characterization, ACS Appl. Mater. Interfaces **45**, 54447 (2021).

[16]J. J. Perez-Grau, J. Cervera, S. Nasir, M. Ali, W. Ensinger, P. Ramirez, and S. Mafe, Additivity of ionic currents in mixed electrolyte solutions and charged conical nanopores, J. Mol. Liq. **360**, 119592 (2022).

[17]J. Cervera, B. Schiedt, R. Neumann, S. Mafe, and P. Ramirez, Ionic conduction, rectification, and selectivity in single conical nanopores, J. Chem. Phys. **124**, 104706 (2006).

[18]M. Queralt-Martin, E. García-Gimenez, S. Mafe, and A. Alcaraz, Divalent cations reduce the pH sensitivity of OmpF channel inducing the pK_a shift of key acidic residues, Phys. Chem. Chem. Phys. **13**, 563 (2011).

[19]M. Queralt-Martin, C. Verdia-Baguena, V. M. Aguilella, and A. Alcaraz, Electrostatic interactions drive the nonsteric directional block of OmpF channel by La^{3+}, Langmuir **29**, 15320 (2013).

[20]M. Emmons-Bell, F. Durant, A. Tung, A. Pietak, K. Miller, A. Kane, C. J Martyniuk, D. Davidian, J. Morokuma, and M. Levin, Regenerative Adaptation to Electrochemical Perturbation in Planaria: A Molecular Analysis of Physiological Plasticity, iScience **22**, 147 (2019).

[21]A. Y. Grosberg, T. T. Nguyen, and B. I. Shklovskii, Colloquium: The physics of charge inversion in chemical and biological systems, Rev. Mod. Phys. **74**, 329 (2002) .

[22]J. Lyklema, Overcharging, charge reversal: Chemistry or physics?, Colloids Surf. A **291**, 3 (2006) .

[23]P. A. Gurnev and S. M. Bezrukov, Inversion of membrane surface charge by trivalent cations probed with a cation-selective channel, Langmuir **28**, 15824 (2012).

[24]Y. He, D. Gillespie, D. Boda, I. Vlassiouk, R. S. Eisenberg, and Z. S. Siwy, Tuning transport properties of nanofluidic devices with local charge inversion, J. Am. Chem. Soc. **131**, 5194 (2009).

[25] X. Wang, Y. Chen, Z. Meng, Q. Zhang, and J. Zhai, Effect of Trivalent "Calcium-like" Cations on Ionic Transport Behaviors of Artificial Calcium-Responsive Nanochannels, J. Phys. Chem. C **122**, 24863 (2018).

[26]K. Xiao, L. Wen, and L. Jiang, Biomimetic Solid-State Nanochannels: From Fundamental Research to Practical Applications, Small **12**, 2810 (2016).

[27]G. Pérez-Mitta, A. G. Albesa, C. Trautmann, M. E. Toimil-Molares, and O. Azzaroni, Bioinspired integrated nanosystems based on solid-state nanopores: "iontronic" transduction of biological, chemical and physical stimuli, Chem. Sci. **8**, 890 (2017).

[28]T. Ma, J.-M. Janot, and S. Balme, Track-Etched Nanopore/Membrane: From Fundamental to Applications, Small Methods **4**, 2000366 (2020).

[29]E. García-Giménez, A. Alcaraz, and V. M. Aguilella, Overcharging below the nanoscale: Multivalent cations reverse the ion selectivity of a biological channel, Phys. Rev. E **81**, 021912 (2010).

[30]P. Apel, Track etching technique in membrane technology, Radiat. Meas. **34**, 559 (2001).

[31]Z. Siwy, D. Dobrev, R. Neumann, C. Trautmann, and K. Voss, Electro-responsive asymmetric nanopores in polyimide with stable ion-current signal, Appl. Phys. A **76**, 781 (2003).

[32]P. Apel, V. Bashevoy, I. V. Blonskaya, and N. E. Lizuno, Shedding light on the mechanism of asymmetric track etching: an interplay between latent track structure, etchant diffusion and osmotic flow, Phys. Chem. Chem. Phys. **18**, 25421 (2016).

[33]P. Ramirez, V. Garcia-Morales, V. Gomez, M. Ali, S. Nasir, W. Ensinger, and S. Mafe, Hybrid circuits with nanofluidic diodes and load capacitors, Phys. Rev. Applied **7**, 064035 (2017).

[34]I. Semenov, S. Raafatnia, M. Sega, V. Lobaskin, C. Holm, and F. Kremer, Electrophoretic mobility and charge inversion of a colloidal particle studied by single-colloid electrophoresis and molecular dynamics simulations, Phys. Rev. E **87**, 022302 (2013).

[35]M. Quesada-Perez, E. Gonzalez-Tovar, A. Martın-Molina, M. Lozada-Cassou, and R. Hidalgo-Alvarez, Overcharging in colloids: beyond the Poisson-Boltzmann approach, ChemPhysChem **4**, 234 (2003).

[36]K. Besteman, M. A. G. Zevenbergen, H. A. Heering, and S. G. Lemay, Direct observation of charge inversion by multivalent ions as a universal electrostatic phenomenon, Phys. Rev. Lett. **93**, 170802 (2004).

[37]J. Pittler,W. Bu, D. Vaknin, A. Travesset, D. J. McGillivray, and M. Lösche, Charge inversion at minute electrolyte concentrations, Phys. Rev. Lett. **97**, 046102 (2006).

[38]W. M. Rosencrans, V. M. Aguilella, T. K. Rostovtseva, and S. M. Bezrukov, α-Synuclein emerges as a potent regulator of VDAC-facilitated calcium transport, Cell Calcium **95**, 102355 (2021).

[39]Z.-Y. Wang and J. Wu, Ion association at discretely-charged dielectric interfaces: Giant charge inversion, J. Chem. Phys. **147**, 024703 (2017).

[40]A. G. Albesa, M. Rafti, and J. L. Vicente, Trivalent cations switch the selectivity in nanopores, J. Mol. Model. **19**, 2183 (2013).

[41]M. Quesada-Perez, A. Martin-Molina, and R. Hidalgo-Alvarez, Simulation of electric double layers undergoing charge inversion: Mixtures of mono and multivalent ions, Langmuir **21**, 9231 (2005) .

[42]S. Mafe, J. A. Manzanares, and P. Ramirez, Modeling of surface vs. bulk ionic conductivity in fixed charge membranes, Phys. Chem. Chem. Phys. **5**, 376 (2003).

[43]M. Fuest, K. K. Rangharajan, C. Boone, A. T. Conlisk, and S. Prakash, Cation dependent surface charge regulation in gated nanofluidic devices, Anal. Chem. **89**, 1593 (2017).

[44] D. Fertig, M. Valiskó, and D. Boda, Rectification of bipolar nanopores in multivalent electrolytes: Effect of charge inversion and strong ionic correlations, Phys. Chem. Chem. Phys. **22**, 19033 (2020).

[45]S. X. Li, W. Guan, B. Weiner, and M. A. Reed, Direct observation of charge inversion in divalent nanofluidic devices, Nanolett. **15**, 5046 (2015).

[46]D. Gillespie, D. Boda, Y. He, P. Apel, and Z. S. Siwy, Biophysical synthetic nanopores as a test case for ion channel theories: The anomalous mole fraction effect without single filing, Biophys. J. **95**, 609 (2008).

[47]W. Nonner and B. Eisenberg, Ion permeation and glutamate residues linked by Poisson-Nernst-Planck theory in L-type calcium channels, Biophys. J. **75**, 1287 (1998).

[48]W. Nonner, L. Catacuzzeno, and B. Eisenberg, Binding and selectivity in L-type calcium channels: a mean spherical approximation, Biophys. J. **79**, 1976 (2000).

[49]G. W. Castellan, Physical Chemistry, Benjamin/Cummings, 1983.

[50]S. Su, Y. Zhang, S. Peng, L. Guo, Y. Liu, E. Fu, H. Yao, J. Du, G. Du, and J. Xue, Multifunctional graphene heterogeneous nanochannel with voltage-tunable ion selectivity, Nat. Commun. **13**, 4894 (2022).

[51]Alcaraz, M. L. López, M. Queralt-Martín, and V. M. Aguilella, Ion Transport in Confined Geometries below the Nanoscale: Access Resistance Dominates Protein Channel Conductance in Diluted Solutions, ACS Nano **11**, 10392 (2017).

[52]D. Stein, M. Kruithof, and C. Dekker, Surface-charge-governed ion transport in nanofluidic channels, Phys Rev Lett. **93**, 035901 (2004).

[53]Y. Green, Effects of surface-charge regulation, convection, and slip lengths on the electrical conductance of charged nanopores, Phys. Rev. Fluids **7**, 013702 (2022).

[54]M. A. Alibakhshi, B. Liu, Z. Xu, and C. Duan, Geometrical control of ionic current rectification in a configurable nanofluidic diode. Biomicrofluidics. **10**, 054102 (2016).

[55]H. C. Chang and G. Yossifon, Understanding electrokinetics at the nanoscale: A perspective, Biomicrofluidics, **3**, 12001 (2009).

[56]J.-P. Hsu, T.-W. Lin, C.-Y. Lin, S. Tseng, Salt-Dependent Ion Current Rectification in Conical Nanopores: Impact of Salt Concentration and Cone Angle, J. Phys. Chem. C, **121**, 28139 (2017).

[57]A. Rojano, A, Córdoba, J. H. Walther, H. A. Zambrano, Effect of charge inversion on nanoconfined flow of multivalent ionic solutions, Phys. Chem. Chem. Phys., **24**, 4935 (2022).

[58]S. Prakash, H. A. Zambrano, K. K. Rangharajan, E. Rosenthal-Kim, N. Vasquez, A. T. Conlisk, Electrokinetic Transport of Monovalent and Divalent Cations in Silica Nanochannels Microfluidics and Nanofluidics, Microfluid. Nanofluid. **20**, 8 (2016).